Oxidative stress enhances and modulates protein *S*-nitrosation in smooth muscle cells exposed to *S*-nitrosoglutathione

E. Belcastro[a, b], W. Wu[a], I. Fries-Raeth[a], A. Corti[b], A. Pompella[b], P. Leroy[a], I. Lartaud[a], C. Gaucher[a]*

[a] *Université de Lorraine, CITHEFOR EA 3452, Faculté de Pharmacie, BP 80403, F-54001 Nancy Cedex, France*

[b] *Department of Translational Research NTMS, University of Pisa Medical School, Via Roma 55, 56126 Pisa, Italy.*

* Corresponding author: Dr Caroline Gaucher. Université de Lorraine, CITHEFOR EA 3452, Faculté de Pharmacie, BP 80403, F-54001 Nancy Cedex, France.

E-mail address: caroline.gaucher@univ-lorraine.fr; Tel.: +33 3 83 68 23 76.

Abstract

Among *S*-nitrosothiols showing reversible binding between NO and -SH group, *S*-nitrosoglutathione (GSNO) represents potential therapeutics to treat cardiovascular diseases (CVD) associated with reduced nitric oxide (NO) availability. It also induces *S*-nitrosation of proteins, responsible for the main endogenous storage form of NO. Although oxidative stress parallels CVD development, little is known on the ability of GSNO to restore NO supply and storage in vascular tissues under oxidative stress conditions.

Aortic rat smooth muscle cells (SMC) were stressed *in vitro* with a free radical generator (2,2'-azobis(2-amidinopropane) dihydrochloride, AAPH). The cellular thiol redox status was reflected through levels of reduced glutathione and protein sufhydryl (SH) groups. The ability of GSNO to deliver NO to SMC and to induce protein *S*-nitrosation (investigated *via* mass spectrometry, MS), as well as the implication of two redox enzymes involved in GSNO metabolism (activity of gamma-glutamyltransferase, GGT, and expression of protein disulfide isomerase, PDI) were evaluated.

Oxidative stress decreased both intracellular glutathione and protein -SH groups (53% and 32% respectively) and caused a 3.5 fold decrease in GGT activity, while PDI expression at the plasma membrane was 1.7-fold increased without any effect on extracellular GSNO catabolism. Addition of GSNO (50 μM) increased protein -SH groups and protein *S*-nitrosation (50%). Mass spectrometry analysis revealed a higher number of proteins *S*-nitrosated under oxidative stress (51 proteins, *vs* 32 in basal conditions) including a higher number of cytoskeletal proteins (17, *vs* 8 in basal conditions) related with cell contraction, morphogenesis and movement. Furthermore, proteins belonging to additional protein classes (cell adhesion, transfer/carrier, and transporter proteins) were *S*-nitrosated under oxidative stress.

In conclusion, higher levels of GSNO-dependent *S*-nitrosation of proteins from the cytoskeleton and the contractile machinery were identified under oxidative stress conditions. The findings may prompt the identification of suitable biomarkers for the appraisal of GSNO bioactivity in treatment of CVD.

Keywords: Oxidative stress, *S*-nitrosoglutathione, Protein *S*-nitrosation, Gamma-glutamyl transferase, Protein disulfide isomerase, Mass spectrometry.

1. Introduction

Cardiovascular diseases like atherosclerosis, pulmonary hypertension, thrombosis, ischemia and cardiac arrhythmia are usually associated with oxidative stress and a reduced bioavailability of nitric oxide (NO) [1]. To overcome this aspect, several NO-related therapeutics have emerged over the past few decades, such as nitrosamines [2], organic nitrates [3], and N-diazeniumdiolates [4]. However, these compounds induce undesirable effects, such as tolerance and hypotension, and are often considered as oxidative stress enhancers in an environment rich in oxygen and/or radical species where they may favour the formation of peroxynitrite ions ($ONOO^-$), a reactive nitrogen species (RNS) producing deleterious proteins nitration [5, 6, 7, 8]. Other NO coumpounds, such as *S*-nitrosothiols may represent safer alternatives [9, 10]. Several investigations on the therapeutic potential of *S*-nitrosothiols have focused on *S*-nitrosoglutathione (GSNO), the physiological storage form of NO in tissues, due to the absence of recorded side effects in preclinical studies [11, 12, 13]. However, even though *S*-nitrosothiols are not prooxidant *per se,* the ability of GSNO to regulate NO bioavailability under oxidative stress conditions has not yet received sufficient attention.

Oxidative stress in the vessel wall has been shown to involve the *tunica media,* where smooth muscle cells (SMC) can produce reactive oxygen species (ROS) – *e.g.* superoxide anion, $O_2^{\bullet-}$ – following the activation of their own NADPH oxidase. SMC probably represent a privileged target of ROS [14]. Exposure of SMC cells to ROS-generating systems actually stimulates migration, proliferation, and growth [15, 16, 17, 18]. SMC also are a main target of (endothelium-derived or exogenous) NO, which exerts in this way its vasorelaxing effects.

NO, besides its direct role in vascular function, also participates in redox signaling by modifying proteins *via S*-nitrosation. The *S*-nitrosation, which is the formation of a covalent bond between NO and the sulfhydryl group of a cysteine residue, is a redox dependent, thiol-

based, reversible posttranslational modification of proteins [19, 20, 21]. There are emerging data suggesting that *S*-nitrosation of proteins plays an important role both in physiology and in a broad spectrum of pathologies [22]. Pathophysiology correlates with hypo or hyper *S*-nitrosation level of specific protein targets. This dysregulation of protein *S*-nitrosation results from a modification of NO availability (quantity and/or localization). NO availability results not only from alterations of the expression, compartmentalization and/or activity of NO synthases, but also reflects the contribution of denitrosylases, including GSNO-metabolizing enzymes, like GSNO reductase releasing GSNHOH, a non active NO-related molecule, and the gamma-glutamyl transferase (GGT) releasing cys-gly-NO, an active NO-related molecule [23]. Redoxines like protein disulfide isomerase (PDI) known to reverse thiol oxidation can also catabolise GSNO to release NO [24].

In the present study, we aimed to assess the suitability and potency of GSNO as a NO donor in an oxidative stress environment. Its metabolism by two specific redox enzymes (GGT and PDI), the cellular thiol redox status and protein *S*-nitrosation were thus analyzed in SMC exposed to oxidative stress induced by a free radical generator, *i.e.* 2,2'-azobis(2-amidinopropane) dihydrochloride (AAPH). We more specifically evaluated whether oxidative stress modulates the bioactivity of GSNO, by favouring release of NO and *S*-nitrosation of potentially critical protein targets related with cell contraction, morphogenesis and movement.

2. Materials and methods

2.1. Materials

2.1.1. Chemicals

All reagents were of analytical grade and all solutions prepared with ultrapure deionized water (>18.2 mΩ.cm). BCA Protein Assay Kit was purchased from Pierce and protease inhibitor cocktail from Roche. The Ez-Link Biotin-HPDP and the high capacity

neutravidin agarose resin were obtained from Fisher Scientific. All other reagents came from Sigma, France country not precised for other companies

2.1.2. Synthesis of S-nitrosoglutathione

GSNO was synthesized as previously described [25]. Briefly, reduced glutathione (GSH) was incubated with an equivalent amount of sodium nitrite under acidic conditions (0.626 M HCl). The concentration of GSNO was calculated using the specific molar absorbance of S-NO bond at 334 nm ($\varepsilon = 922\ M^{-1}cm^{-1}$) and the Beer Lambert Law.

2.2. Cell culture and oxidative stress model

Vascular smooth muscle cells derived from embryonic rat aorta (A-10 line, ATCC, USA) were grown in Dulbecco's modified Eagle's medium supplemented with 10% (v/v) fetal bovine serum, 4.5 g/L glucose, 2% (v/v) glutamine (200 mM), 100 U/mL penicillin, 100 µg/mL streptomycin, 1 mM sodium pyruvate, as well as phenol red. They were cultured at 37°C under 10% (v/v) CO_2 in a humidified incubator and used between passages 25 and 30. For all experiments, cells were seeded in a 6-wells plate at 6,400 cells/cm^2, 48 h before stimulation. Oxidative stress was induced on cells during 2 h at 37°C by addition of 50 mM of 2,2'-azobis(2-amidinopropane) dihydrochloride (AAPH) in an incubation medium containing 5% (v/v) fetal bovine serum, 4.5 g/L glucose, 2% (v/v) glutamine (200 mM), 100 U/mL penicillin and 100 µg/mL streptomycin. After oxidative stress induction, 50 µM of GSNO (or the same volume of PBS) was added for an additional incubation period of 1 h at 37°C.

In another set of experiments, 15 min before the end of oxidative stress induction, 20 mM of serine borate complex (SBC), or 100 µM of bacitracin were added to inhibit GGT or PDI, respectively.

2.3. S-nitrosoglutathione metabolism

2.3.1. Quantification of extracellular S-nitrosothiols

After cell incubation (see section 2.2.), media were collected for quantification of nitrite ions and total *S*-nitrosothiols (including residual GSNO) using the Griess and Griess-Saville methods. Briefly, 100 µL of sample were diluted with 100 µL acetoacetic solution (pH= 2.5). Then, for nitrite ions quantification, 40 µL of sulfanilamide solution in 0.4 M HCl were added (Griess assay). For *S*-nitrosothiols quantification, the sulfanilamide solution was supplemented with 0.2% (w/v) $HgCl_2$ (to cleave the S-NO bond: Griess-Saville assay). Finally, the diazonium salt formed was reacted with 10 µL of a 0.6% (w/v) N-(1-naphthyl) ethylenediamine solution to form a chromophoric azo product that absorbs at 540 nm. To calculate the concentration of *S*-nitrosothiols, free nitrite ions quantified by Griess assay were subtracted from those obtained with the Griess-Saville assay.

2.3.2. Quantification of intracellular S-nitrosothiols

Intracellular *S*-nitrosothiols were quantified using the DAN fluorescent probe (lower limit of quantification than the Griess method). After incubation (see section 2.2.), cells were washed with PBS and lysed with 500 µL of 0.4% (m/v) Triton X-100 in 0.1 M HCl. The intracellular *S*-nitrosated proteins were quantified by the DAN (nitrite ions) or DAN-Hg^{2+} (*S*-nitrosothiols) using standard curves (0.1 - 1 µM) of sodium nitrite and GSNO, respectively [26]. The concentration of nitrite ions (DAN) was subtracted from the DAN-Hg^{2+} quantification to obtain the intracellular *S*-nitrosothiols concentration, which was normalized upon the intracellular proteins concentration (see section 2.7).

2.4. Thiol redox status

The redox potential of the culture medium was measured by using a redox electrode (Hanna Instruments) combined with a reference Ag/AgCl electrode, (E = 0.207 V)**.**

2.4.1. Quantification of reduced membrane thiols

After incubation, media were withdrawn and cells washed twice (PBS). Cells were then incubated for 10 min in the dark with 750 µL of 1 mM 5-5'-dithio-bis(2-nitrobenzoic) acid (DTNB) prepared in PBS. Then, 200 µL from each well were transferred in triplicate in a 96-wells plate and absorbance read at 405 nm (EL800, Universal Microplate Reader, Biotek Instruments). Membrane thiols concentration was calculated using a GSH standard curve ranging from 3.25 µM to 32.5 µM and expressed relatively to protein quantity (see section 2.7).

2.4.2. Quantification of intracellular reduced glutathione

Intracellular GSH was measured as previously described [27, 28], with some adaptations. Cells were lysed in a cold 3.3 % (v/v) perchloric acid solution and centrifuged for 15 min at 10,000 × *g*. Acidic supernatants were neutralized with 10 M NaOH and diluted 10 times in 0.1 M HCl containing 2 mM EDTA. Sixty µL of diluted samples or standard GSH solutions (0.65–3.25 µM) were transferred to a 96-wells plate; 120 µL of 0.4 M borate buffer (pH= 9.2) and 20 µL of 5.4 mM 2,3-naphthalene dicarboxaldehyde (NDA) solution prepared in ethanol were then added into each well. Microplate was incubated 25 min on ice in the dark. The fluorescence intensity of GSH-NDA adducts was measured using a microplate reader (Synergy 2 model, Biotek Instruments, Colmar, France) with excitation set at 485 ± 20 nm and emission at 528 ± 20 nm and expressed relatively to protein quantity (see section 2.7).

2.4.3. Quantification of intracellular protein reduced thiols

Intracellular protein reduced thiols were quantified using the DTNB method. After treatments, cells were lysed in a 3.3% (v/v) cold perchloric acid solution and centrifuged for 15 min at 10,000 × *g*. The pellets were resuspended in PBS containing 0.5% (V/V) sodium dodecylsulfate (SDS). Cells were then incubated 10 min in the dark with 700 µL of 1 mM DTNB. After incubation, 200 µL were transferred in triplicate in a 96-wells plate and the absorbance was read at 405 nm. Intracellular thiols concentration was calculated using a GSH standard curve ranging from 3.25 µM to 32.5 µM and expressed relatively to protein quantity (see section 2.7).

2.5. Determination of gamma-glutamyltransferase activity

Gamma-glutamyl transferase activity was kinetically determined using the synthetic GGT substrate L-ɣ-glutamyl-3-carboxy-4-nitroanilide (GCNA). After treatments, incubation media were replaced with 750 µL of 1 mM of GCNA in 100 mM Tris buffer (pH= 7.4) containing 20 mM glycyl-glycine and 10 mM $MgCl_2$, with/without 50 mM AAPH or 20 mM of the GGT inhibitor serine-borate complex (SBC). Cells were then incubated at 37°C, and 50 µL of incubation medium were transferred in a 96-wells plate each 30 min and absorbance read at 405 mm. At the end of the kinetic assay, cells were lysed in 500 µL 0.1 M HCl containing 0.4% (m/v) Triton X-100 for protein quantification (see section 2.7).

2.6. Cell membrane PDI expression

Cells were scrapped in 50 mM Tris buffer (pH= 8) added with 50 mM 2-mercaptoethanol and protease inhibitor cocktail. After 30-min incubation on ice, cell lysates were centrifuged at 17,600 × *g* during 20 min. The pellet containing membrane proteins was ressuspended in 50 mM Tris buffer (pH= 8) added with 1% (v/v) SDS and agitated for 30 min on ice. Membrane proteins were then centrifuged for 20 min at 21,000 × *g*. Finally, proteins

were precipitated with 100% cold acetone for 1 h at -20°C. After centrifugation (3,000 × *g*, 10 min), the pellet was ressuspended in 50 mM Tris-HCl buffer (pH= 6.8) containing 0.15 M NaCl, 1% (w/v) SDS and 1% (w/v) Triton X-100. Proteins were quantified (see section 2.7) and 10 µg were deposited on a SDS PAGE with 10% separative gel and 4% concentrating gel. After migration, proteins were transferred on a polyvinylic membrane and labelled with anti-PDI (sc-20132 Santa Cruz biotechnology) or anti-actin antibody diluted 1/1000 or 1/2000, respectively. Secondary antibody conjugated with HRP (sc-2004, Santa Cruz biotechnology) diluted 1/5000 was used to quantify PDI/Actin ratio using Image J 1.47V software (NIH, USA).

2.7. Total protein quantification

Protein determination was performed using the Pierce BCA Protein Assay Kit, following instructions of the manufacturer. A standard curve ranging from 0.025 to 1 mg.mL^{-1} was built with bovine serum albumin to calculate protein concentration.

2.8. Purification and identification of S-nitrosated proteins

Cells incubated in a-75 cm^2 flask were lysed in 500 µL of 50 mM Tris (pH= 6.8) containing 0.15 M NaCl, 1% (v/v) NP-40, 0.1% (v/v) SDS, 1 mM EDTA, 0.1 mM neocuproine and protease inhibitor cocktail. *S*-nitrosated proteins were purified by the biotin switch technique as previously described [29, 30], with some adaptations. Briefly, free thiols in cell lysates were blocked with 50mM of *N*-ethylmaleimide (NEM). Then, *S*-nitrosated proteins were labeled with pyridyl disulfide-biotin (*N*-[6-(biotinamido)hexyl]-3'-(2'-pyridyldithio)-propionamide biotin, biotin-HPDP) after cutting the S-NO bond with sodium ascorbate. Biotin-HPDP-labeled proteins were purified with NeutrAvidin beads (High Capacity NeutrAvidin Agarose Resin) and eluted in a buffer containing 1.5% (v/v) 2-mercaptoethanol.

After purification, *S*-nitrosated proteins were identified by mass spectrometry, as follows. Samples diluted 4-fold in 6 M urea, 50 mM Tris (pH= 8.0) were processed for cysteine reduction and alkylation, followed by overnight digestion in 10 vol of 50 mM Tris (pH= 8.0), 1 mM $CaCl_2$ containing 100 ng sequencing-grade trypsin (Promega). Protein digests were purified through C18 mini spin columns (Pierce, Thermofisher scientific, France), resuspended in 8 µL of 2% (v/v) acetonitrile, 0.1% (v/v) trifluoroacetic acid and analyzed through label-free LC-MALDI as previously described [31]. Proteins and peptides were identified based on fragmentation spectra by interrogation of the whole Swissprot database through the public Mascot server (taking in account protein scores above 80.0 and peptide scores above 20.0 at first rank, allowing one trypsin miscleavage and considering cysteine carbamidomethylation and methionine oxidation as optional). Finally, identified proteins were classified using the Panther database [32].

2.9. Statistical analysis of data

Results are expressed as means ± standard error of the mean (sem). Statistical analyses were performed using either the Student t-test (for enzyme activity/expression or inhibition) or two-way ANOVA ($p_{condition}$ basal *versus* AAPH, $p_{treatment}$ with or without GSNO and $p_{interaction}$ between condition and treatment) followed by a Bonferroni's multiple comparisons test. The GraphPad Prism software (GraphPad Software version 5.0, San Diego, USA) was used.

3. Results

3.1. Oxidative stress biomarkers

A 3-h incubation of SMC in presence of 50 mM AAPH significantly increased the redox potential of the culture medium from 256 ± 19 (basal) to 484 ± 8 mV (AAPH) (n = 3, Student t test, $p < 0.05$ *vs* basal). Addition of GSNO (50 µM) during the final 1-h incubation

had no impact on this redox potential, neither in control nor under AAPH exposure. No variation of the pH (7.4) was observed all along the experiment.

Under oxidative stress, the GGT activity decreased 3.5 fold, from 1.35 ± 0.20 to 0.39 ± 0.14 nmol/min/mg of proteins (n = 3, Student t test, $p < 0.05$). At variance, PDI localization at the plasma membrane increased 1.7 fold, from 0.72 ± 0.02 to 1.22 ± 0.31 (PDI/actin ratio, n = 4, Student t test, $p < 0.05$).

The intracellular GSH content significantly decreased with oxidative stress **(Fig. 1-A**), while extracellular GSH increased **(Fig. 1-B)** ($p_{condition} < 0.0001$ for both). The addition of GSNO produced a very slight (1.9 %) but significant increase in extracellular GSH ($p_{treatment} = 0.0395$), both in basal and oxidative conditions ($p_{interaction}$ ns), while this did not permit and recover intracellular levels of GSH, which remained at a low value under AAPH exposure ($p_{treatment}$ and $p_{interaction}$ ns, **Fig. 1-A**).

Reduced thiols at the plasma membrane (0.015 ± 0.002 nmol/µg of proteins) did not change with oxidative stress. Intracellular protein thiols evolved differently according to conditions and treatment ($p_{interaction} < 0.0001$, **Fig. 1-C)**. They decreased with oxidative stress in the absence of GSNO. The addition of GSNO under oxidative stress almost doubled the intracellular protein thiol.

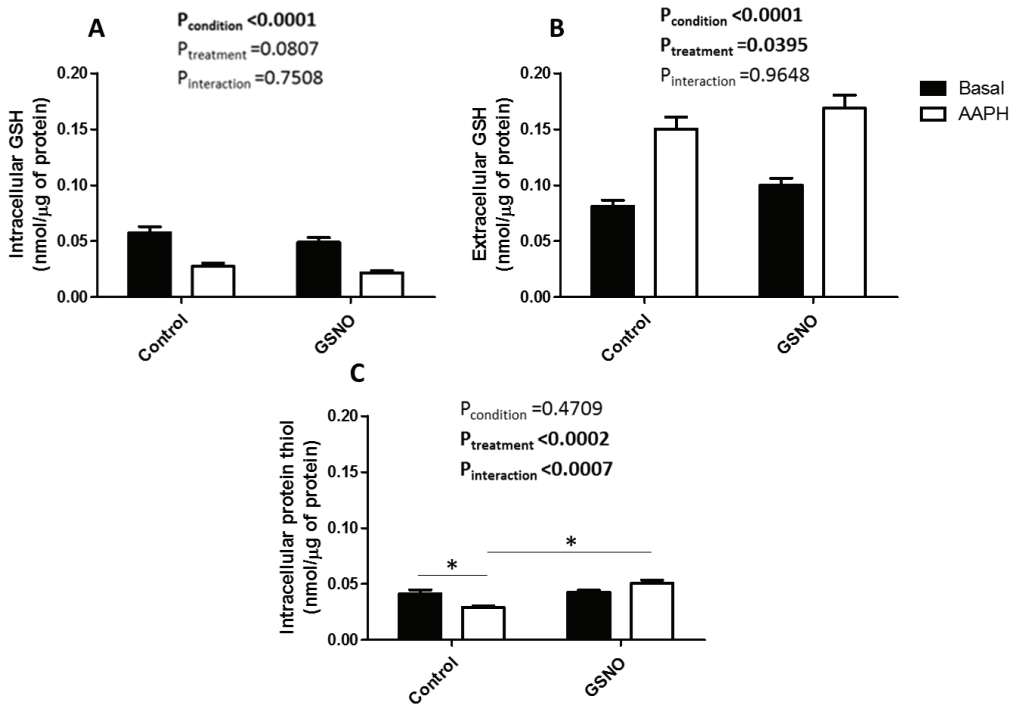

Fig. 1. Intracellular and extracellular thiol status in basal and oxidative stress conditions. Smooth muscle cells were incubated for a total of 3 h without (basal) or with 50 mM AAPH. In each condition, 50 µM GSNO or GSNO+AAPH were added during the 3rd h of incubation. Intracellular reduced thiols **(C)** were quantified by reacting precipitated proteins with DTNB. Intracellular **(A)** and extracellular GSH **(B)** were quantified with the NDA probe in the supernatant after protein precipitation. Results are presented as means ± sem of three independent experiments and compared using a two way ANOVA ($p_{condition}$ (Basal *vs* AAPH), $p_{treatment}$ (Control, GSNO) and $p_{interaction}$); * $p<0.05$ (Bonferroni's multiple comparisons test).

3.2. Extracellular GSNO metabolism and intracellular formation of S-nitrosothiols.

After one hour in contact with cells, only approx. 20 µM of GSNO **(Fig. 2-A)** – out of the 50 µM initially added, and approx. 12 µM of nitrite ions **(Fig. 2-B)** were found in the extracellular space, indicating that GSNO is partly metabolized by SMC to release NO (detected as nitrite ions).

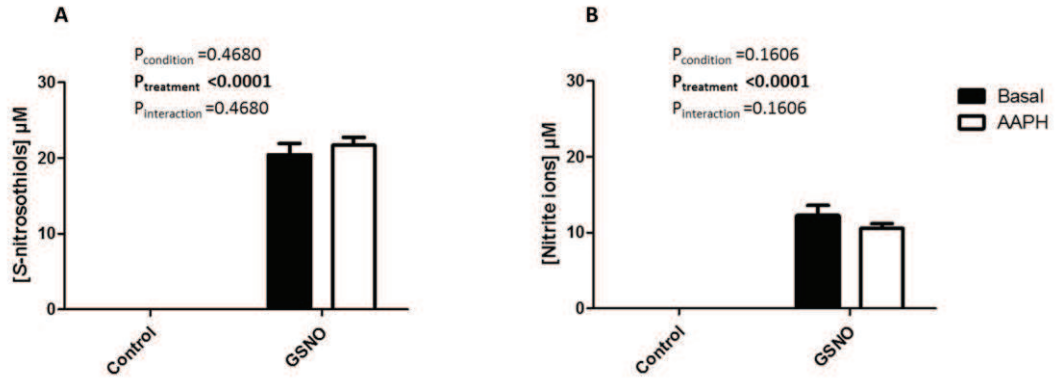

Fig. 2. Extracellular metabolism of *S*-nitrosoglutathione. Smooth muscle cells were incubated for 3 h without (Basal) or with 50 mM AAPH. In each condition, 50 µM GSNO or GSNO+AAPH were added during the 3rd hour of incubation. *S*-nitrosothiols **(A)** and nitrite ions **(B)** were quantified by the Griess-Saville and Griess methods, respectively. Results are presented as means ± sem of three independent experiments and compared using a two way ANOVA ($p_{condition}$ (Basal *vs* AAPH), $p_{treatment}$ (Control, GSNO) and $p_{interaction}$).

GGT and PDI inhibition under basal conditions led to an increased extracellular content of GSNO to 27 ± 0.5 µM for SBC and 28 ± 0.5 µM for bacitracin ($p<0.05$ *versus* GSNO in the absence of inhibition, t-test) and a decrease in extracellular nitrite ions concentrations (10 ± 0.4 µM for SBC ($p>0.05$) and 7 ± 0.9 µM for bacitracin ($p<0.05$ *versus* GSNO in the absence of inhibition, t-test), attesting a decrease in GSNO catabolism. Similar profiles were obtained with GGT and PDI inhibition under oxidative stress.

At the intracellular level, addition of GSNO for 1 hour induced formation of *S*-nitrosothiols, which nearly doubled under oxidative stress compared to basal condition **(Fig. 3)**. Both enzymes were implicated in the formation of intracellular *S*-nitrosothiols in both conditions. Inhibition of GGT by SBC led to a half time decrease in the content of *S*-nitrosothiols, both in basal condition ($2.1.10^{-4} \pm 0.2.10^{-4}$ nmol/ µg of proteins, $p<0.05$ *versus* GSNO in the absence of inhibition, t-test) and under oxidative stress ($6.6.10^{-4} \pm 0.4.10^{-4}$ nmol/ µg of proteins, $p<0.05$ *versus* GSNO in the absence of inhibition, t-test). PDI inhibition by bacitracin showed the same profile with a *S*-nitrosothiols formation decreasing to $2.90.10^{-4} \pm 0.05.10^{-4}$ nmol/µg of proteins in basal condition ($p < 0.05$ *versus* GSNO in the absence of

inhibition, t-test) and to 0.00045 ± 0.00005 nmol/ µg of proteins under oxidative stress ($p<0.05$ *versus* GSNO in the absence of inhibition, t-test).

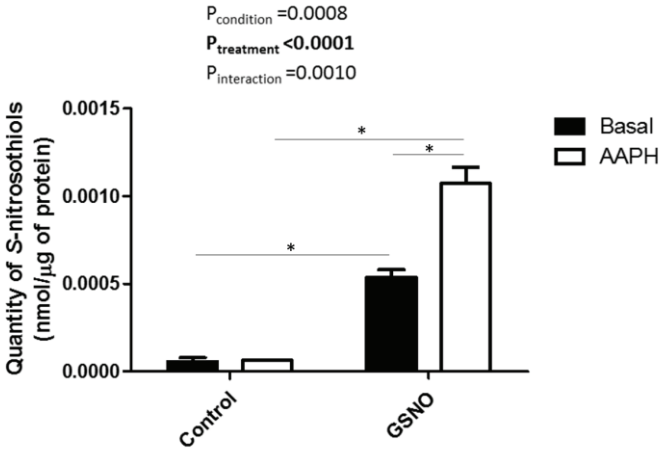

Fig. 3. Intracellular formation of *S*-nitrosothiols. Intracellular *S*-nitrosothiols were quantified by the DAN/Hg^{2+} method after incubation of smooth muscle cells for 3 h without (Basal) or with 50 mM of AAPH. In each condition, 50 µM GSNO or GSNO+AAPH were added during the 3rd hour of incubation. Results are presented as means ± sem of three independent experiments and compared using a two way ANOVA ($p_{condition}$ (Basal *vs* AAPH), $p_{treatment}$ (Control, GSNO) and $p_{interaction}$); * $p<0.05$ (Bonferroni's multiple comparisons test).

3.3. Identification of S-nitrosated proteins

Purification and identification of proteins undergoing *S*-nitrosation revealed that 32 proteins were nitrosated under basal conditions, whereas 51 were *S*-nitrosated under oxidative stress. GSNO-nitrosated proteins were mainly present in macromolecular complexes and organelles under basal conditions, while the membrane and extracellular region pools were prevailing under oxidative stress **(Table 1)**.

Table 1. Distribution of *S*-nitrosated proteins among distinct cell compartments upon treatment with GSNO (50 µM) of smooth muscle cells cultured under basal or oxidative stress (50 mM AAPH) conditions.

	Percentage of total identified proteins	
Cell compartment	**Basal + GSNO**	**AAPH + GSNO**
Cell junction		2.20
Membrane		43.50
Macromolecular complex	48	2.20
Extracellular matrix		2.20
Cytosol	8	6.50
Organelle	44	2.20
Extracellular region		41.30

The identified proteins belonged to 20 different classes for basal conditions, and to 23 for oxidative stress. Three additional classes were *S*-nitrosated by GSNO under oxidative stress, designed as cell adhesion, transfer/carrier and transporter proteins **(Fig. 4).** Among these classes, importin subunit beta-1 and procollagen c-endopeptidase enhancer 1, involved in the cellular cycle and proliferation of vascular smooth muscle cells, respectively [33, 34], have been identified.

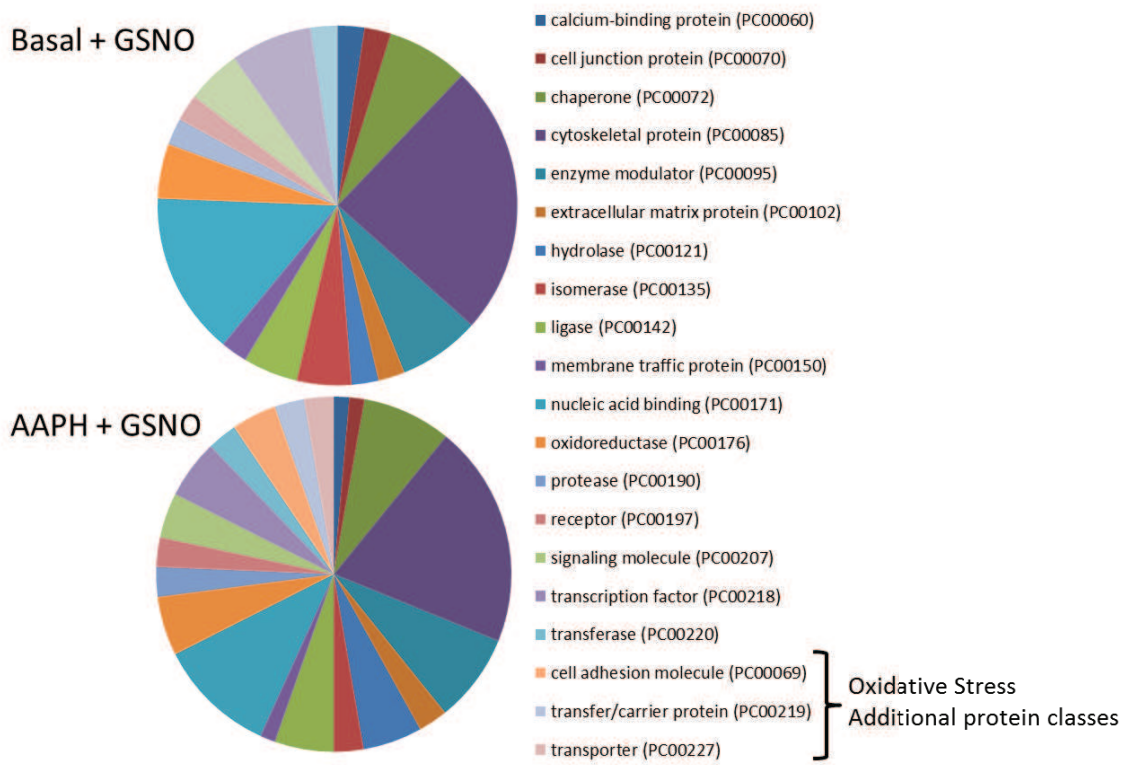

Fig. 4. Identification and classification of smooth muscle cells proteins *S*-nitrosated in basal or oxidative stress conditions. Proteins were *S*-nitrosated by 50 µM GSNO in cells exposed or not to oxidative stress (50 mM AAPH). After purification (biotin switch technique), proteins identified by mass spectrometry were classified using the Panther database.

In both culture conditions, the two major classes of *S*-nitrosated proteins were nucleic acid binding transcription factors and cytoskeletal proteins. Nucleic acid binding transcription factors accounted for 15% of identified proteins in basal conditions – with 6 different proteins – and 11% of identified proteins under oxidative stress, with 8 different proteins including elongation factor 2 or cellular nucleic acid-binding protein. *S*-nitrosoglutathione induced *S*-nitrosation of a high proportion of SMC contractile proteins: 8 different cytoskeletal proteins were identified in basal conditions, and additional 9 (total: 8 + 9 = 17) under oxidative stress. Such proteins are structural constituents of cytoskeleton variably implicated in muscle contraction, as well as in cell morphogenesis and movement **(Table 2).**

Table 2. Molecular function and biological implications of cytoskeletal proteins *S*-nitrosated by 50 μM GSNO under basal or oxidative stress conditions.

Basal + GSNO	GSNO + AAPH		
Panther family/subfamily		**Molecular function**	**Biological process**
	Elongation Factor 1-Gamma	Structural constituent of cytoskeleton	Cell communication
Actin, Aortic Smooth Muscle			Movement and morphogenesis and organization Mitosis
Alpha-Actinin-1		Structural constituent of cytoskeleton Actin binding	Movement
Calponin-2			Movement and morphogenesis and organization
Filamin-A			
	Filamin-B		Muscle contraction
Filamin-C			Movement and morphogenesis and organization
	Inverted Formin-2		Muscle contraction Movement
	Lipoma-Preferred Partner	Structural constituent of cytoskeleton	
Myosin Light Polypeptide 6			Morphogenesis and organization
	Pdz And Lim Domain Protein 5	Structural constituent of cytoskeleton Actin binding	Movement and morphogenesis Muscle contraction
	Tropomyosin	Motor activity Structural constituent of cytoskeleton	Morphogenesis and organization
	Talin-1	Structural constituent of cytoskeleton	Movement, organization and morphogenesis Mitosis
	Transgelin	Structural constituent of cytoskeleton Actin binding	Movement, organization and morphogenesis Muscle contraction
	Tubulin Beta-2a Chain	Structural constituent of cytoskeleton	
Lim Domain And Actin-Binding Protein 1			Movement, Morphogenesis, Organization
Pdz And Lim Domain Protein 5			Movement, organization and morphogenesis Muscle contraction

4. Discussion

The present study was designed to evaluate the bioactivity of GSNO in vascular SMC exposed to oxidative stress. Experiments were thus planned in order to assess the efficiency of GSNO-dependent NO release, and to verify possible quantitative/qualitative changes induced by oxidative conditions in cellular protein *S*-nitrosation.

From an experimental point of view, two main approaches can be used to induce oxidative stress, *i.e.* either by inhibiting cellular antioxidant defenses or by increasing the free radical load. The latter can be obtained by exposing cells to extracellular ROS like $O_2^{\bullet-}$ or H_2O_2. Prolonged enzymatic generation of $O_2^{\bullet-}$ can be sustained *e.g.* by the xanthine/xanthine oxidase system, which however can introduce a major bias in the results, as itself can denitrosate *S*-nitrosothiols [35]. H_2O_2 prooxidant effects are mediated by the formation of hydroxyl radical, $^{\bullet}OH$, through the transition metal-catalyzed Fenton reaction. However, metal cations are also known to catalyze direct degradation of *S*-nitrosothiols, preventing its use in our study. On the other hand, the water soluble azo compound 2,2'-azobis (2-amidinopropane) dihydrochloride (AAPH) can be considered as a 'clean' and reproducible free radical generator, as it spontaneously decomposes at 37°C into one mole of nitrogen and two moles of carbon-centered radicals. AAPH-derived radicals can either combine with each other to produce a stable product, or react with molecular oxygen to generate peroxyl radicals ($ROO^{\bullet}$), or with polyunsaturated lipids of cell membranes thus starting lipid peroxidation [36]. A number of studies have employed AAPH to investigate antioxidant defenses in cellular systems [37, 38]. More recently, cytotoxic and genotoxic effects of $ROO^{\bullet}$ originating downstream of AAPH have been studied in a human microvascular endothelial cell line [39]. The effects of oxidative stress on the development of the cardiovascular system were also investigated after administration of AAPH in the air chamber of chicken embryos [40]. As far as SMC are concerned, AAPH was used to study the direct effects of free radicals on cyclic

AMP-related cholesterol homeostasis [41]. On this background, the exposure of vascular SMC to AAPH was chosen as a simple and reproducible model of oxidative stress.

AAPH-induced oxidative stress caused no significant change in the extracellular GSNO metabolism, as the consumption of added GSNO and the corresponding NO release were largely the same in both conditions. In principle, the GSNO degradation might ensue from a direct oxidation by AAPH radicals. However, when checked in the absence of cells, the direct AAPH-mediated oxidation of GSNO (50 μM) actually released 4 ± 0.1 μM nitrite ions, *i.e.* much less than the concentrations detected in the presence of SMC (18.3 ± 0.6 μM), suggesting that most of the observed GSNO metabolism in oxidative stress conditions in SMC occurs through the activity of diverse cellular enzymes.

Oxidative stress induced a remarkable increase in the formation of intracellular *S*-nitrosothiols under GSNO addition, a finding whose interpretation requires additional considerations. GGT is a critical enzyme in GSNO metabolism [42], essential for the release of NO and its subsequent utilization in *S*-nitrosothiols formation. Indeed, intracellular concentrations of *S*-nitrosothiols detected within GGT inhibition were markedly decreased. However, even if the GGT activity was decreased by oxidative stress, it was still implicated in the same extent in GSNO extracellular catabolism and intracellular *S*-nitrosothiols formation. Actually, GGT inhibition did not entirely suppress GSNO metabolism, as it could not restore the initial extracellular concentration of GSNO: approx. 26 μM GSNO were detected at the end of the incubation with GGT inhibitor, *vs* 50 μM initially added. Taken together, these findings indicate that GGT activity is certainly involved in the extracellular metabolism of GSNO, but other enzymes must also be implicated in the process. As regards PDI, its inhibition produced similar results: enzyme inhibition did not entirely suppress GSNO extracellular metabolism and approx. 28 μM GSNO (of 50 μM initially added) were still detectable in the extracellular compartment at the end of incubation. Cellular GGT and PDI

activities appear therefore to stay implicated in GSNO catabolism, even if they were inversely (GGT activity decreases, while PDI expression at the membrane level increases) impacted by oxidative stress.

The observed increase in *S*-nitrosation of SMC proteins under oxidative stress conditions was rather unexpected, as prooxidants should oxidize reduced thiols to disulfides and/or other sulfur species, which are then unavailable for nitrosation. The oxidation of thiols during oxidative stress might prevent *S*-nitrosation thus interfering with NO-based physiologic signaling [43]. However, it has also been showed that *S*-nitrosation is a protection of thiols from oxidation by NO [44].

In our experiments, oxidative stress (in the absence of added GSNO) caused both a decrease in intracellular GSH and a decrease in SH groups in cellular proteins, accompanied by an increase in extracellular GSH. The latter was likely the result of the AAPH-induced decrease in GGT activity at the SMC plasma membrane level, resulting in a lower consumption of extracellular GSH. In fact, the AAPH-induced decrease of GGT activity can be explained as the effect of either direct inactivation of the enzyme protein by AAPH radicals or the large increase in the extracellular redox potential. Direct oxidation of plasma membrane proteins by AAPH is a known phenomenon [45]. Loss of cellular GGT activity was also reported following exposure of lung epithelial cells to hyperoxia-induced lipid peroxidation [46], and indeed, AAPH is itself known to induce lipid peroxidation [47].

The decrease of protein SH groups induced by AAPH was reversed by GSNO (**Fig. 1-C**). In principle, the addition of GSNO in an oxidative stress environment would rather be expected to enhance oxidative stress by production of peroxynitrite anions. In our systems, no peroxynitrite ion was detected in smooth muscle cells in basal conditions upon GSNO addition, using DHR probe. AAPH-induced oxidative stress increased the intracellular peroxynitrite ion concentration up to 6.7 ± 0.8 μM; however, the concomitant addition of

GSNO did not modify peroxynitrite ion concentration (5.9 ± 0.4 μM). The protection offered by GSNO to intracellular protein -SH groups could be explained by the release of GSH concomitantly to the release of NO. Released GSH can be incorporated in the intracellular GSH pool to support GSH-dependent antioxidant defenses. However, our data did not show any recovery of intracellular GSH levels after GSNO addition. This phenomenon was probably due to direct oxidation of GSH by AAPH challenge. Furthermore, our data showed that GSNO is able to recover the oxidation of protein thiols caused by oxidative stress (**Fig. 1-C**). In this perspective, the ability of GSNO to protect reduced protein thiols from oxidative stress, making them again available to react with NO, may represent the mechanism explaining the increased formation of intracellular *S*-nitrosothiols (**Fig. 3**) observed under oxidative conditions.

Protein *S*-nitrosation is considered as an important mechanism for post-translational modulation of protein function, and several studies have described such modulatory effects on a series of cys-containing proteins, being potential targets of RNS-dependent nitrosative modifications [48, 49, 50]. In addition to direct modulation of protein function, protein *S*-nitrosation can also represent a mean for constitution of 'NO stores' in tissues. Indeed, different studies support the idea that *S*-nitrosation of tissue thiols is a mechanism for the constitution of local reservoirs from which biologically active NO can be subsequently released [51, 52, 53]. Identification and assessment of such NO stores could provide a valuable biomarker for evaluation of the therapeutic efficiency of NO donors.

The increase in *S*-nitrosation mostly concerned proteins belonging to plasma membrane and extracellular region, which is not surprising considering that the AAPH-dependent oxitative challenge was originated in the extracellular compartment. In particular, the detailed pattern of *S*-nitrosated proteins indicates that most of the proteins selectively *S*-nitrosated under oxidative stress conditions are of primary relevance for the performance of

SMC functions, which are often altered in vascular diseases, such as cell communication, cytoskeletal organization, contraction, morphogenesis and movement.

Interestingly, the pathway involves actin cytoskeleton dynamics of several key regulatory proteins including Calponin-2 (CNN2), Myosin Light Polypeptide 6 (MYL6), Transgelin (TAGLN) and Lipoma Preferred Partner (LPP). The role of *S*-nitrosation in regulating these proteins is not completely understood particularly during oxidative stress. Each of these proteins has been shown to play a role in regulating and modulating smooth muscle contraction or nitric oxide signaling. *In vitro S*-nitrosation of skeletal muscle myosin, for example, increases the force of the actomyosin interaction while decreasing its velocity indicating a relaxed state [54]. The calcium binding protein CNN2 has been shown to participate in regulating smooth muscle contraction by binding to actin, calmodulin, troponin C and tropomyosin. The interaction of calponin with actin inhibits the actomyosin Mg-ATPase activity [55, 56]. This tonic inhibition of the ATPase activity of myosin in smooth muscle is blocked by Ca^{2+}-calmodulin, which inhibits CNN2 actin binding [57]. MYL6 regulates light chain of myosin and it does not bind calcium, but it is always involved in muscle contraction and skeletal muscle tissue development. Transgelin (also designated SM22α and p27) is a smooth muscle protein that physically associates with cytoskeletal actin filament bundles in contractile smooth muscle cells. Studies in transgelin knockout mice have demonstrated a pivotal role for transgelin in the regulation of Ca^{2+} independent contractility [58] and it is proposed to be necessary for actin polymerization and bundling [59]. Moreover, LPP, a nucleocytoplasmic shuttling protein, is located in focal adhesions and associates with the actin cytoskeleton [60]. LPP can function as an adaptor protein that constitutes a platform that orchestrates protein-protein interactions and contributes to the migratory phenotype of SMC [61]. As ROS have also been shown to enhance cell migration [62, 63] and GSNO has

been shown to decrease smooth muscle cells migration capacity [64], we can speculate that LPP *S*-nitrosation could protect against oxidative stress induced cell migration.

Therefore, considered together, all these proteins, almost quite implicated in Ca^{2+}-dependent contractility and in NO signalling, constitute a potential interactome and discovering their behavior as *S*-nitrosated proteins may further help our understanding of several processes, such as contraction-relaxation signaling of SMC or their phenotype switching, in the vascular system.

In conclusion, our study documented that oxidative stress can significantly modify smooth muscle cells metabolism of GSNO an endogenous NO-donor presently under active investigation as a potential therapeutic agent. In particular, oxidative stress was shown to increase the extent, and profoundly modify the pattern of GSNO-dependent protein *S*-nitrosation, with the additional involvement in the process of several proteins critical for SMC homeostasis and function. These data can represent a valuable basis for the identification of biomarkers of GSNO bioactivity in the vascular system, as well as for the appraisal of possible beneficial effects of this NO donor in the treatment of cardiovascular diseases.

Acknowledgments

We thank the proteomics plateform (Dr Jean-Baptiste Vincourt) from the Federation de Recherche (FR3209 CNRS - BMCT) based at the Biopôle on the biology-health campus at Université de Lorraine for identification of S-nitrosated proteins (LC-MALDI MS).

Funding

This work was supported by the *Université de Lorraine* and the *Région Lorraine* (UHP_2011_EA3452_BMS_0062, RL 21/11, RL 140/12, CPER 2007-13 PRST « Ingénierie Moléculaire et Thérapeutique – Santé »). Programme VINCI 2014 – Université Franco Italienne, project number C2-56.

References

[1] Maron BA, Tang S-S, Loscalzo J. S-Nitrosothiols and the S-Nitrosoproteome of the Cardiovascular System. Antiox Redox Signal. 2012, 18: 270-287.

[2] Messin R, Boxho G, De Smedt J, Buntinx IM. Acute and chronic effect of molsidomine extended release on exercise capacity in patients with stable angina, a double-blind crossover clinical trial versus placebo, J. Cardiovasc. Pharmacol. 1995, 25: 558-563.

[3] Bennett BM. Biotransformation of organic nitrates and vascular smooth muscle cell function, Trends Pharmacol. Sci. 1994, 15: 245-249.

[4] Morley D, Keefer LK. Nitric oxide/nucleophile complexes: a unique class of nitric oxide-based vasodilators, J. Cardiovasc. Pharmacol. 1993, 22: S3-S9.

[5] Kowaluk EA, Poliszczuk R, Fung HL. Tolerance to relaxation in rat aorta: comparison of an S-nitrosothiol with nitroglycerin, Eur. J. Pharmacol. 1987, 144: 379–383.

[6] Butler AR, Glidewell C, McGinnis J, Bisset WI. Further investigations regarding the toxicity of sodium nitroprusside, Clin. Chem. 1987, 33: 490–492.

[7] Henry PJ, Drummer OH, Horowitz JD. S-nitrosothiols as vasodilators: implications regarding tolerance to nitric oxide-containing vasodilators, Br. J. Pharmacol. 1989, 98: 757–766.

[8] van Heerden PV, Sviri S, Ilett KF, Lam CF. Inhaled diazeniumdiolates (NONOates) as selective pulmonary vasodilators, Expert Opin. Investig. Drugs 2002, 11: 897–909.

[9] Al-Sa'doni H, Ferro A. S-nitrosothiols: a class of nitric oxide-donor drugs, Clin Sci 2000, 98: 507–520.

[10] Ricardo KF, Shishido SM., de Oliveira MG, Krieger MH. Characterization of the hypotensive effect of S-nitroso-N-acetylcysteine in normotensive and hypertensive conscious rats, Nitric Oxide 2002, 7: 57–66.

[11] de Belder AJ, MacAllister R, Radomski MW., Moncada S, Vallance PJ. Effects of S-nitrosoglutathione in the human forearm circulation: evidence for selective inhibition of platelet activation, Cardiovasc. Res. 1997, 28: 691–694.

[12] Radomski MW, Rees DD, Dutra A, Moncada S. S-Nitroso-glutathione inhibits platelet activation in vitro and in vivo, Br. J. Pharmacol. 1992, 107: 745–749.

[13] Langford EJ, Brown AS, Wainwright RJ, Debelder AJ, Thomas MR, Smith REA, Radomski MW, Martin JF, Moncada S. Inhibition of platelet activity by S-nitrosoglutathione during coronary angioplasty, Lancet 1994, 344: 1458–1460.

[14] Rajagopalan S, Kurz S, Münzel T, Tarpey M, Freeman BA, Griendling KK, Harrison DG. Angiotensin II-mediated hypertension in the rat increases vascular superoxide production via membrane NADH/NADPH oxidase activation. Contribution to alterations of vasomotor tone, J Clin Invest. 1996, 97(8):1916-23.

[15] Kunsch C, Medford RM. Oxidative stress as a regulator of gene expression in the vasculature, Circ. Res. 1999, 85: 753–766.

[16] Irani K. Oxidant signaling in vascular cell growth, death, and survival: a review of the roles of reactive oxygen species in smooth muscle and endothelial cell mitogenic and apoptotic signaling, Circ. Res. 2000, 87: 179–183.

[17] Griendling KK, Sorescu D, Ushio-Fukai M. NAD(P)H oxidase: role in cardiovascular biology and disease, Circ. Res. 2000, 86: 494–501.

[18] Rao GN and Berk BC. Active oxygen species stimulate vascular smooth muscle cell growth and proto-oncogene expression, Circ. Res. 1992, 70: 593–599.

[19] Foster MW, Hess DT, Stamler JS. Protein S-nitrosylation in health and disease: a current perspective, Trends Mol Med. 2009, 15: 391-404.

[20] Paige JS, Xu G, Stancevic B, Jaffrey SR. Nitrosothiol reactivity profiling identifies S-nitrosylated proteins with unexpected stability, Chem Biol. 2008, 15:1307-1316.

[21] Gow AJ, Chen Q, Hess DT, Day BJ, Ischiropoulos H, Stamler JS. Basal and stimulated protein S-nitrosylation in multiple cell types and tissues, J Biol Chem. 2002, 277: 9637-9640.

[22] Hsieh HJ, Liu CA, Huang B, Tseng AH, Wang DL. Shear-induced endothelial mechano transduction: the interplay between reactive oxygen species (ROS) and nitric oxide (NO) and the pathophysiological implications, J Biomed Sci, 2014, 21:3.

[23] Dahboul F, Leroy P, Maguin Gate K, Boudier A, Gaucher C, Liminana P, Lartaud I, Pompella A, Perrin-Sarrado C. Endothelial γ-glutamyltransferase contributes to the vasorelaxant effect of S-nitrosoglutathione in rat aorta, PLoS One. 2012, 7(9):e43190.

[24] Gaucher C, Boudier A, Dahboul F, Parent M, Leroy P. S-nitrosation/Denitrosation in Cardiovascular Pathologies: Facts and Concepts for the Rational Design of S-nitrosothiols. Curr. Pharm. Des. 2013, 19:000-000.

[25] Parent M, Dahboul F, Schneider R, Clarot I, Maincent P, Lerroy P, Boudier A. A complete physicochemical identity card of S-nitrosoglutathione, Curr Pharm Anal 2013; 9: 31–42.

[26] Wu W, Gaucher C, Diab R, Fries I, Xiao YL, Hu XM, Maincent P, Sapin-Minet A. Time lasting S-nitrosoglutathione polymeric nanoparticles delay cellular protein S-nitrosation, Eur J Pharm Biopharm. 2015, 89:1-8.

[27] Lewicki K, Marchand S, Matoub L, Lulek J, Coulon J, Leroy, P. Development of a fluorescence based microtiter plate method for the measurement of glutathione in yeast, Talanta 2006, 70, 876–882.

[28] Maguin Gaté K, Lartaud I, Giummelly P, Legrand R, Pompella A, Leroy P. Accurate measurement of reduced glutathione in gamma-glutamyltransferase-rich brain microvessel fractions, Brain Res. 2011, 1369: 95-102.

[29] Jaffrey SR, Snyder SH. The biotin switch method for the detection of S-nitrosylated proteins, Sci STKE 2001, 86: pl1.

[30] Jaffrey SR. Detection and characterization of protein nitrosothiols, Methods Enzymol. 2005, 396: 105-118.

[32] Riffault M, Moulin D, Grossin L, Mainard D, Magdalou J, Vincourt JB. Label-free relative quantification applied to LC-MALDI acquisition for rapid analysis of chondrocyte secretion modulation, J Proteomics. 2015, 114: 263-273.

[32] Mi H, Poudel S, Muruganujan A, Casagrande JT, Thomas PD. PANTHER version 10: expanded protein families and functions, and analysis tools, Nucleic Acids Res. 2016, 44: D336-D342.

[33] Jiyuan Chen, Kathleen M. Maltby, Joseph M. Miano. A novel retinoid-response gene set in vascular smooth muscle cells, Biochem Biophys Res Commun. 2001, 28 (2):475-482.

[34] Kanaki T, Morisaki N, Bujo H, Takahashi K, Ishii I, Saito Y. The regulatory expression of procollagen COOH-terminal proteinase enhancer in the proliferation of vascular smooth muscle cells, Biochem Biophys Res Commun. 2000, 270(3):1049-54.

[35] Trujillo M, Alvarez MN, Peluffo G, Freeman BA, Radi R. Xanthine oxidase-mediated decomposition of S-nitrosothiols. J Biol Chem. 1998, 273: 7828-7834.

[36] Noguchi N, Takahashi M, Tsuchiya J, Yamashita H, Komuro E, Niki E. Action of 21-aminosteroid U74006F as an antioxidant against lipid peroxidation. Biochem Pharmacol. 1998, 55: 785-91.

[37] Yang JH, Park JW. Oxalomalate, a competitive inhibitor of $NADP^+$-dependent isocitrate dehydrogenase, enhances lipid peroxidation-mediated oxidative damage in U937 cells, Arch Biochem Biophys. 2003, 416(1):31-7.

[38] Aldini G, Carini M, Piccoli A, Rossoni G, Facino RM. Procyanidins from grape seeds protect endothelial cells from peroxynitrite damage and enhance endothelium-dependent relaxation in human artery: new evidences for cardio-protection, Life Sci. 2003, 73: 2883-2898.

[39] Scarpato R, Gambacciani C, Svezia B, Chimenti D, Turchi G. Cytotoxicity and genotoxicity studies of two free-radical generators (AAPH and SIN-1) in human microvascular endothelial cells (HMEC-1) and human peripheral lymphocytes, Mutat Res. 2011, 722(1):69-77.

[40] He RR, Li Y, Li XD, Yi RN, Wang XY, Tsoi B, Lee KK, Abe K, Yang X, Kurihara H.A new oxidative stress model, 2,2-azobis(2-amidinopropane) dihydrochloride induces cardiovascular damages in chicken embryo, PLoS One. 2013; 8:e57732.

[41] Gesquiere L, Loreau N, Blache D. Role of the cyclic amp-dependent pathway in free radical induced cholesterol accumulation in vascular smooth muscle cells, Free Radic Biol Med. 2000, 29(2):181–190.

[42] Angeli V, Tacito A, Paolicchi A, Barsacchi R, Franzini M, Baldassini R, Vecoli C, Pompella A, Bramanti E. A kinetic study of gamma-glutamyltransferase (GGT)-mediated S-nitrosoglutathione catabolism, Arch Biochem Biophys. 2009, 481(2): 191-6.

[43] Adachi T, Weibrod RM, Pimentel DR, Ying J, Sharov VS, Schoneich C, Cohen RA. S-glutathiolation by peroxynitrite activates SERCA during arterial relaxation by nitric oxide, Nat Med. 2004, 10:1200–120.

[44] Sun J, Steenbergen C, Murphy E.S-nitrosylation: NO-related redox signaling to protect against oxidative stress, Antioxid Redox Signal. 2006, 8:1693-1705.

[45] Soszyński M, Bartosz G. Decrease in accessible thiols as an index of oxidative damage to membrane proteins, Free Rad. Biol. Med. 1997, 23: 463-9.

[46] van Klaveren RJ, Pype JL, Demedts M, Nemery B. Decrease in gamma-glutamyltransferase activity in rat type II cells exposed in vitro to hyperoxia: effects of the 21-aminosteroid U-74389G, Exp Lung Res. 1997, 23(4):347-59.

[47] Niki E. Free radical initiators as source of water- or lipid-soluble peroxyl radicals, Methods Enzymol. 1990, 186 100-108.

[48] Huang B, Chen SC, Wang DL. Shear flow increases S-nitrosylation of proteins in endothelial cells, Cardiovasc. Res. 2009, 83:536–546.

[49] Hoffmann J, Dimmeler S, Haendeler J. Shear stress increases the amount of S-nitrosylated molecules in endothelial cells: important role for signal transduction, FEBS Letters 2003, 551:153–158.

[50] Marshall HE, Merchant K, Stamler JS. Nitrosation and oxidation in the regulation of gene expression. Faseb J. 2000, 14:1889–1900.

[51] Sarr M, Chataigneau M, Etienne-Selloum N, Diallo AS, Schott C, Geffard M, Stoclet JC, Schini-Kerth VB, Muller B. Targeted and persistent effects of NO mediated by S-nitrosation of tissue thiols in arteries with endothelial dysfunction, Nitric Oxide. 2007, 17(1):1-9.

[52] Alencar JL, Lobysheva I, Chalupsky K, Geffard M, Nepveu F, Stoclet JC, Muller B. S-nitrosating nitric oxide donors induce long-lasting inhibition of contraction in isolated arteries, J. Pharmacol. Exp. Ther. 2003, 307:152-9.

[53] Wu W, Perrin-Sarrado C, Ming H, Lartaud I, Maincent P, Hu XM, Sapin-Minet A, Gaucher C. Polymer nanocomposites enhance S-nitrosoglutathione intestinal absorption and promote the formation of releasable nitric oxide stores in rat aorta, Nanomedicine. 2016, pii: S1549-9634(16)30053-3.

[54] Evangelista AM, Rao VS, Filo AR, Marozkina NV, Doctor A, Jones DR, Gaston B, Guilford WH. Direct regulation of striated muscle myosins by nitric oxide and endogenous nitrosothiols, PLoS One, 2010, 5: e11209.

[55] Carmichael JD, Winder SJ, Walsh MP, Kargacin GJ. Calponin and smooth muscle regulation, Can J Physiol Pharmacol, 1994, 72: 1415–1419.

[56] Winder SJ, Allen BG, ClementChomienne O, Walsh MP. Regulation of smooth muscle actinmyosin interaction and force by calponin., Acta Physiol Scand, 1998, 164: 415–426.

[57] Mezgueldi M, Mendre C, Calas B, Kassab R, Fattoum A. Characterization of the regulatory domain of gizzard calponin. Interactions of the 145–163 region with Factin, calcium binding proteins, and tropomyosin. J Biol Chem. 1995, 270: 8867–8876.

[58] Je HD, Sohn UD. SM22alpha is required for agonistinduced regulation of contractility: evidence from SM22alpha knockout mice, Mol Cells, 2007, 23: 175–181.

[59] Han M, Dong LH, Zheng B, Shi JH, Wen JK, Cheng Y. Smooth muscle 22 alpha maintains the differentiated phenotype of vascular smooth muscle cells by inducing filamentous actin bundling, Life Sci. 2009, 84(13-14):394-401.

[60] Petit MM, Fradelizi J, Golsteyn RM, Ayoubi TA, Menichi B, Louvard D, Van de Ven WJ, Friederich E. LPP, an actin cytoskeleton protein related to zyxin, harbors a nuclear export signal and transcriptional activation capacity. Mol Biol Cell, 2000, 11: 117–129.

[61] Gorenne I, Jin L, Yoshida T, Sanders JM, Sarembock IJ, Owens GK, Somlyo AP, Somlyo AV. LPP expression during in vitro smooth muscle differentiation and stent-induced vascular injury, Circ Res. 2006, 98:378-385.

[62] Kim J, Min G, Bae YS, Min DS. Phospholipase D is involved in oxidative stress-induced migration of vascular smooth muscle cells via tyrosine phosphorylation and protein kinase C, Exp Mol Med. 2004, 36:103–109.

[63] Jin L, Kern MJ, Otey CA, Wamhoff BR, Somlyo AV. Angiotensin II, focal adhesion kinase, and PRX1 enhance smooth muscle expression of lipoma preferred partner and its newly identified binding partner palladin to promote cell migration, Circ Res 2007, 100:817–825.

[64] Simmers P, Gishto A, Vyavahare N, Kothapalli CR. Nitric oxide stimulates matrix synthesis and deposition by adult human aortic smooth muscle cells within three-dimensional cocultures, Tissue Eng Part A. 2015, 21:1455-1470.